Annals of Biomedical Engineering, Vol. 22, pp. 202–211, 1994
Printed in the USA.

0090-6964/94 $10.50 + .00

Comparison of Electrical Transients and Corrosion Responses of Pulsed MP35N and 316LVM Electrodes

LISA W. RIEDY and JAMES S. WALTER

The Rehabilitation Research and Development Center, Hines VA Hospital, Hines, IL

Abstract—Functional neuromuscular stimulation (FNS) is often limited by electrode malfunctions such as corrosion and breakage, particularly for intramuscular and epimysial type electrodes. As a result, the electrochemical charge injection characteristics and corrosion responses of single strand 316LVM stainless steel and MP35N nickel-cobalt alloy electrodes were evaluated *in vitro*. For charge balance, capacitor coupled monophasic protocols with varying charge injections were employed. Electrodes were evaluated with either positive-first or negative-first pulses, 60 Hz, 100 μsec pulse duration, and stimulation periods from 100 to 240 hours. Charge injection densities ranged from 20 to 80 μC/cm^2. For both anodic-first and cathodic-first pulsing, the potential transients for the MP35N electrodes were more extreme than for the 316LVM electrodes over the test period, and increased corrosion was apparent on the MP35N electrodes from both optical and scanning electron microscopy. Therefore, 316LVM, but not MP35N, may be suitable for FNS applications with charge injection densities less than 40 μC/cm^2.

Keywords—Neuroprosthetics, Electrode corrosion, 316LVM stainless steel, MP35N nickel-cobalt alloy, Electrical transients.

INTRODUCTION

Peripheral applications of intramuscular and epimysial implantable electrodes for functional neuromuscular stimulation (FNS) have gained widespread acceptance. These electrodes are used in the treatment of many neurological disorders including bladder dysfunctions, respiratory dysfunction and limb paralysis (1,8,11,13,27). Despite this widespread acceptance, their use continues to be limited by electrode malfunctions such as corrosion and breakage (10,12,18).

To avoid corrosion and breakage problems of implantable electrodes and cables, two electrode types are generally used (3,19,25,27,31). The first type of electrode is constructed with one metal for both the insulated lead portion and the exposed stimulating portion of the electrode. Typically, 316LVM and MP35N are substrates used. The advantages include easy manufacturing, low cost, and the ability to implant the electrode percutaneously (12). The disadvantages include a low charge injection limit and the need for a large surface area for corrosion resistance. The second type consists of electrodes constructed of two different metals for the insulated lead portion and the exposed stimulating electrode. Although the second type of FNS electrodes have the advantages of using corrosion-resistant platinum disks for the stimulating surface and flexible stainless steel wire for the lead portion, there exist disadvantages of using dissimilar metals (27). These include the introduction of galvanic corrosion and the need for more involved fabrication. Due to the disadvantages of dissimilar metal electrodes, there is a need to characterize further the stimulation conditions for single metal electrodes.

As electrode materials, 316LVM stainless steel and MP35N nickel-cobalt alloy electrodes offer excellent mechanical strength for a single metal electrode (18,20). These materials are readily obtained as well as being fairly inexpensive (18,20). However, these electrode materials may be susceptible to pitting corrosion during pulsing (12). Several studies have indicated conditions under which corrosion begins by identifying a relationship between charge injection, the maximum anodic potential [E_{max}(A)] and the corrosion response (2). From these studies, the maximum limit of safe charge injection for cathodic stimulating wave forms is generally reported to be 40 μC/cm^2, although lower limits have been suggested (16). A safe charge injection limit for anodic-first pulsing is not clearly defined for either alloy; however, anodic pulsing is known to be more corrosive than cathodic-first pulsing (12). One of the electrical transients associated with pulsing and corrosion responses is E_{max}. This transient is associated with charge transfer and faradaic reactions and is measured as the maximum potential excursion following the initial access potential. E_{max}(A) values versus a standard calomel reference electrode greater than 1.2 V have been associated with corrosion responses (12).

Despite these guidelines, the onset of corrosion for

Acknowledgment—We acknowledge the support of Dr. Stuart Cogan, Head Material Scientist, EIC Laboratories, for his extensive discussion of electrode corrosion analysis and review of this manuscript. We also acknowledge the support of this study by the VA Rehabilitation Research & Development (Rehab. R&D) Service, Merit Review (B658-R) and the Hines VA Hospital, Rehabilitation R&D Center.

Address correspondence to Lisa W Riedy, VA Hines Hospital, Rehabilitation R&D Center (151L), P.O. Box 20, Hines, IL 60141.

(Received 22Jul93, Revised 9Dec93, Accepted 9Dec93)

pulsed 316LVM and MP35N electrodes remains uncertain. This uncertainty is associated with 1) the relatively short time course of previous studies; 2) the use of end point evaluations of corrosion rather than repeated measures over time; and 3) the use of an inappropriate *in vitro* electrolyte environment (12,14,21). For these reasons, we developed: 1) long-time course studies: 2) intermediate corrosion response evaluations, and 3) a minimal *in vitro* bath, without protein, glucose, or urea, based on the *in vivo* interstitial environment (22,23,32). Electrical transient data and corrosion responses for both anodic-first as well as cathodic-first pulses are presented for continuous pulsing up to ten days.

METHODS

The single strand 316LVM and MP35N wires (7 mil, 0.17 mm in diameter) were supplied by ESPI Inc. (Agoura, CA). Both alloys were in the annealed condition with tensile strengths of 670 MPa and 980 MPa for 316LVM and MP35N, respectively. The percent composition of the 316LVM metal included 17 Cr, 12 Ni, 2.5 Mo, and Fe balance. For the MP35N metal, the percent composition was 0.0006 C, 0.02 Mn, 0.003 P, 0.001 S, 0.02 Si, 20.49 Cr, 34.75 Ni, 9.70 Mo, 0.65 Ti, 33.97 Co, and 0.50 Fe. For both metals, percent composition was determined by ESPI Inc. and was in good agreement with reported values (12,20).

After insulating the wires in silastic tubing, epoxy was used to seal the interface. All electrodes were then cut to an exposed length of 3 mm. Electrodes were cleaned by dipping in acetone for 5 minutes, wiping with tissue paper, and then rinsing with distilled water. Electrodes were evaluated *in vitro* using charge injection protocols similar to those used *in vivo* (30). A buffered *in vitro* electrolyte solution, representative of interstitial fluid (7), was used, consisting of 29 mM bicarbonate ($NaHCO_3$ 2.44 g/L), 3 mM phosphate (Na_2HPO_4 2.39 g/L and NaH_2PO_4 0.08 g/L) and 137 mM NaCl (8.00 g/L), purged with 5% CO_2, 6% O_2 and 89% N_2 gas to a final pH of 7.4 (9).

All experiments were conducted using the stimulating circuit shown in Fig. 1A. A Frederick Haer 6i stimulator (Brunswick, ME) with an internal resistance of 20 KΩ was used. A 5 KΩ resistor and diode were added to the output of the stimulator to help maintain constant current stimulating conditions and charged balanced pulses. The time constant (TC) of the discharge circuit was calculated from the product of the capacitance (0.47 μF) and the resistance of the discharge circuit, which consisted of the sum of the access resistance of the electrodes, the 1.8 KΩ shunt resistor and the 100 Ω current sensing resistor (Fig. 1A) (6). This TC was determined to 0.96 msec and was found to provide complete discharge as well as charge balance in the current record within 4 ms for all charge injection densities used.

Monophasic, anodic-first and cathodic-first current pulses were applied in a 3-electrode test cell which was comprised of the test electrode, a large surface area Pt counter electrode (4 cm of 1 mm diameter wire), and a saturated calomel reference electrode (SCE) in close proximity to the test electrode (Fig. 1A). The stimulation pro-

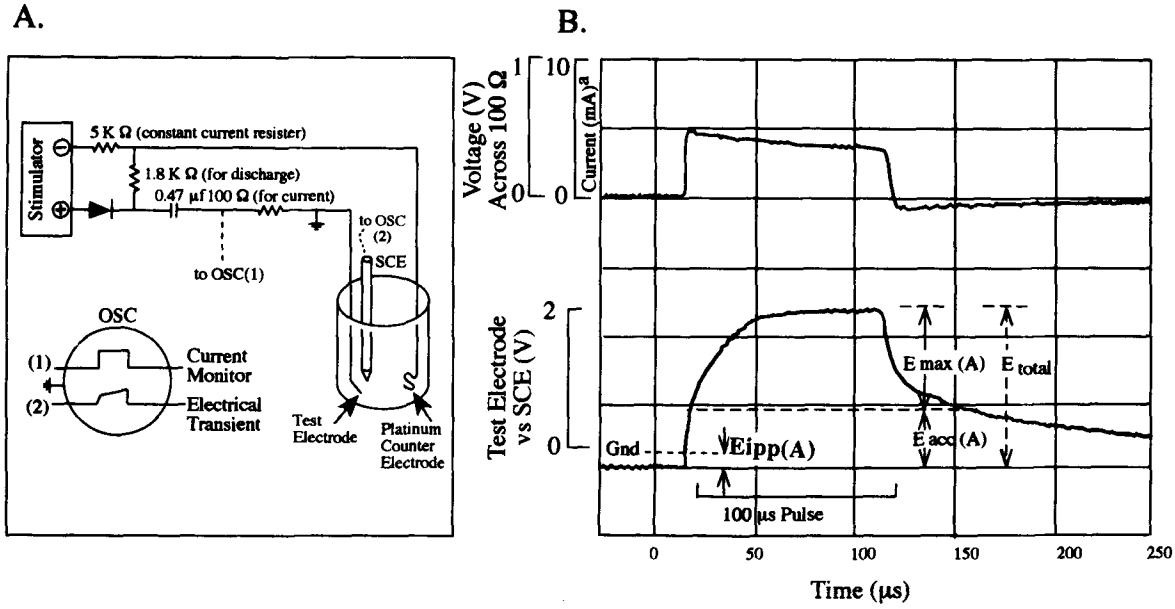

FIGURE 1. (A) Stimulating circuit consisting of 0.47 μF capacitor, 1.8 KΩ shunt resistor and 100 Ω current sensing resistor was used for all experiments with anodic-first pulsing. For cathodic-first pulsing, the polarity was changing at the stimulator. (B) Represents a typical electrical transient obtained for electrodes stimulated with anodic-first pulsing with a current of 7.5 mA. Electrical transient parameters (E_{ipp}, E_{acc}, E_{max}, and E_{tot}) are as illustrated.

tocol consisted of 100 μs pulses at a repetition rate of 60 pps and was conducted until electrode dissolution was apparent, or for up to 240 hours. MP35N electrodes and 316LVM electrodes were stimulated at charge injection densities of 80, 40 and 20 μC/cm^2 (15.0, 7.5, and 3.8 mA) and 80 and 40 μC/cm^2, respectively. A charge injection density of 20 μC/cm^2 was not used with the 316LVM electrodes due to the limited corrosion response at 40 μC/cm^2. A 100 MHz storage oscilloscope (Tektronix model 2232) equipped with 10X probes (Tek P6109) resulting in 10 MΩ impedance was used for recording electrical transients. As shown in Fig. 1B, for anodic pulsing; the maximum anodic potential [E_{max}(A)] was obtained by subtracting the access voltage [E_{acc}(A)] from the maximum anodic voltage excursion (E_{tot}). The access resistance (Ra) was obtained from the voltage transient by dividing E_{acc} by the instantaneous current. The values obtained for Ra were slightly less than E_{acc} directly divided by the listed currents (3.8, 7.5, or 15.0 mA) due to a 5–10% drop off in the current during the 100 μsec pulse (Fig. 1B). The interpulse potential (E_{ipp}) was measured just prior to the onset of the pulse and represents the shift from ground potential.

The corrosion response of each electrode was periodically checked throughout the stimulation period. This evaluation required removing the electrodes from the buffered electrolyte, soaking them for 30 minutes in distilled water to remove any salt crystals before observation under the light microscope. With this analysis, light microscopy provided the time course monitoring of each electrode's corrosion response. SEM was used to confirm the final corrosion response of each electrode. A loss of the natural shiny metal surface is referred to as tarnishing as seen with light microscopy. Appearance of surface disruptions and pitting (as observed by SEM only) are referred to as roughening. A flaking in the metal surface is described as scaling, and dissolution describes a loss in electrode material, typically seen as a decrease in electrode length.

RESULTS

Figure 2 shows a more severe corrosion response for an MP35N electrode compared with that of a 316LVM electrode during 240 hours of anodic pulsing at 40 μC/cm^2. Initially, both alloys were shiny with wire drawing marks visible with light microscopy. However, after 120 hours of stimulation, the 316LVM electrode was only tarnished, whereas the MP35N electrode was visibly scaled. Additional stimulation did not result in a significant change in the corrosion response of either electrode, showing the greater overall corrosion of MP35N compared to 316LVM.

Electrical transient components (E_{acc}, E_{max}, E_{tot}, and E_{ipp}) were all found to increase during anodic pulsing at 40

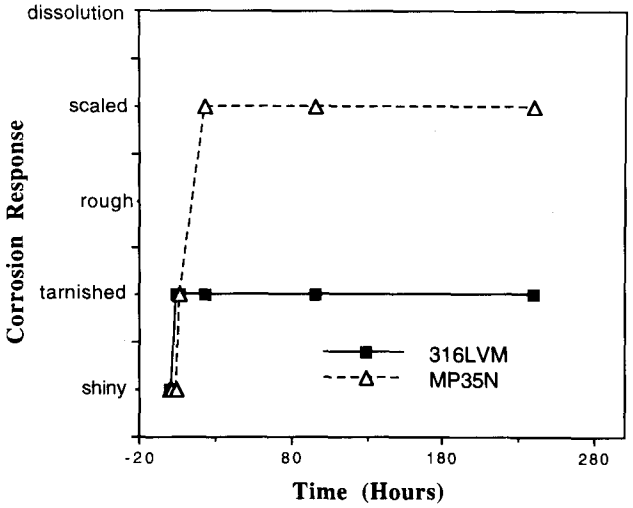

FIGURE 2. Corrosion responses of 316LVM and MP35N electrodes pulsed anodic-first at 40 μC/cm^2.

μC/cm^2 (Figs. 3A–C) correlating with the corrosion responses. Of these, E_{acc} was found to be the most sensitive to corrosion. After 240 hours of stimulation, there was a three-fold increase in E_{acc} for the 316LVM electrode and a four-fold increase for the MP35N electrode (Fig. 3A). E_{max} values for 316LVM increased by 1.37 V and for MP35N by 1.39 V after 240 hours of stimulation (Fig. 3B). The greatest proportional differences between MP35N and 316LVM were observed for E_{ipp} values. The E_{ipp} values for MP35N were driven to become roughly two to four times more negative than observed for 316LVM (Fig. 3C).

In addition to evaluating the electrodes with anodic pulsing at 40 μC/cm^2, MP35N electrodes were evaluated using 80 and 20 μC/cm^2; 316LVM electrodes were evaluated using 80 μC/cm^2 (Table 1). At 80 μC/cm^2, increased corrosion was observed for both metals proportional to the doubling of the charge injection density. The MP35N electrode continued to show accelerated corrosion with scaling visible after seven hours of stimulation, whereas the 316LVM electrodes only showed signs of tarnishing. Although a safe charge injection limit of 40 μC/cm^2 for 316LVM is generally recommended to avoid corrosion, it was necessary to decrease the charge injection to 20 μC/cm^2 for the MP35N electrodes to avoid active corrosion with 240 hours of anodic-first pulsing. Despite this low charge injection density for MP35N, after 144 hours of stimulation, the electrode was tarnished; after an additional 52 hours of stimulation, roughening of the electrode's surface was observed.

The effect of charge injection on the corrosion response of anodically pulsed MP35N electrodes, as observed under SEM, is illustrated in Fig. 4A–C. As expected, the most severe corrosion response occurred at the highest charge injection density of 80 μC/cm^2 (Fig. 4C). Exten-

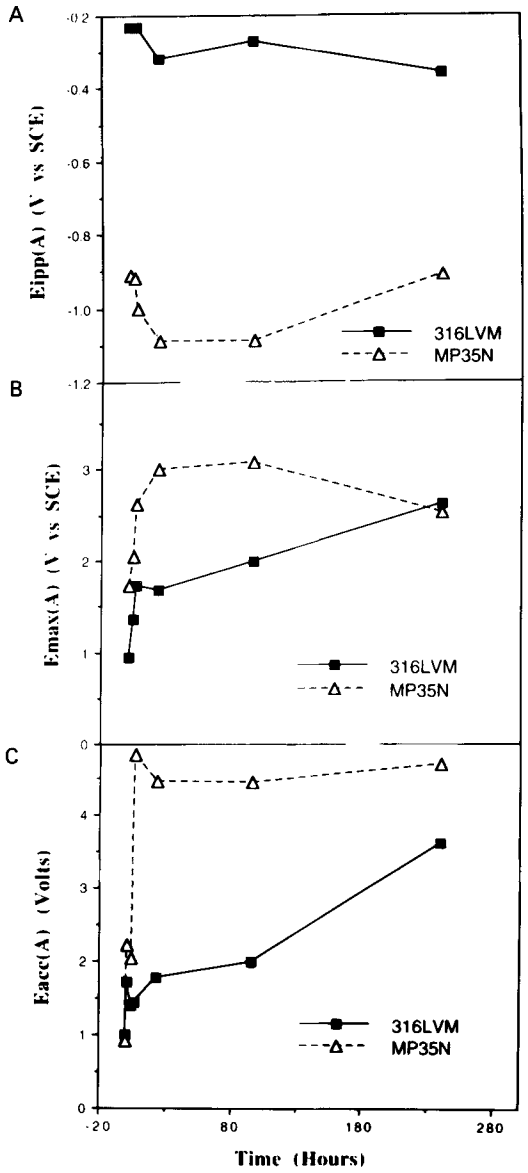

FIGURE 3. Changes in (A) E_{acc}, (B) E_{max}, and (C) E_{ipp} over time for 316LVM and MP35N electrodes pulsed anodic-first at 40 μC/cm².

sive surface disruptions, including scaling and pitting, along with dissolution at the tip, were observed across the entire electrode's surface. At 40 μC/cm², the degree of surface disruption was considerably reduced (Fig. 4B). To a lesser extent, scaling and pitting were still visible at this charge injection; however, electrode dissolution did not occur. At the lowest charge injection density of 20 μC/cm², scaling was no longer apparent and only small pits were noticeable (Fig. 4A).

In addition to the corrosion response, electrical transients were recorded for anodic pulsing at the different charge injection densities. At the highest charge injection of 80 μC/cm², E_{acc} increased the most over the course of stimulation for both alloys. Of the two alloys, the largest increases were observed for the 316LVM electrode, which increased by 10.67 V compared with an increase of only 8.14 V for MP35N. During the same stimulation period, E_{max} values were observed to fluctuate for both alloys, with an overall increase observed at the end of the stimulation period (Table 1). The sum of E_{acc} and E_{max} is E_{tot} and is listed in Table 1. E_{tot} showed fewer fluctuations than E_{acc} and E_{max} individually, and consistently increased during pulsing. E_{ipp} values changed little during the pulsing period with the exception of the 316LVM electrode stimulated at a charge injection of 80 μC/cm². At this charge injection, dissolution of the 316LVM electrode occurred, at which point the E_{ipp} values became very negative. Overall, E_{ipp} values were larger for the MP35N electrodes than for the 316LVM electrodes. At the lowest charge injection density of 20 μC/cm² for the MP35N electrode, the electrical transient components decreased, which correlated with a decrease in corrosion. Despite this reduced charge injection density (20 μC/cm²), E_{acc}, E_{max}, and E_{ipp} increased over the course of stimulation by 1.46 V, 1.24 V, and 0.57 V, respectively.

Effects of cathodic pulsing on 316LVM and MP35N electrodes were also evaluated. In general, the corrosion responses were considerably reduced for any given charge injection density using cathodic-first pulsing rather than anodic-first pulsing for both alloys (Table 2). As expected, cathodic pulsing at the highest charge injection of 80 μC/cm² resulted in the most severe corrosion response, with greater corrosion observed for the MP35N electrode. At this level of charge injection, roughening of the 316LVM electrode's surface was observed, while scaling of the MP35N electrode's surface was observed after 240 hours of stimulation. As the charge injection was decreased to 40 μC/cm², the differences in the corrosion responses of 316LVM and MP35N electrodes were more apparent. Roughening and pitting were evident on the MP35N electrode, while only tarnishing was observed on the 316LVM electrode. Due to this corrosion response of the MP35N electrode at 40 μC/cm², the charge injection was further decreased to 20 μC/cm². Even at this low level of charge injection, the electrode's surface appeared tarnished after 240 hours of cathodic-first pulsing.

A representative SEM comparison of the corrosion responses for MP35N and 316LVM electrodes stimulated at 40 μC/cm² with cathodic-first pulsing is shown in Fig. 5A–B. After 240 hours of stimulation, pitting and surface roughening were apparent on the MP35N electrode (Fig. 5A), as indicated by the arrowheads on the SEM, but only wire drawing marks were visible on the 316LVM electrode (Fig. 5B).

Electrical transients (E_{max}, E_{acc}, E_{tot}, and E_{ipp}) with the cathodic-first pulsing were monitored over time for both alloys at each charge injection level (Table 2). At 80 μC/

TABLE 1. Electrical transients for anodic-first pulses for 316LVM and MP35N electrodes

	Time (Hrs)	E_{acc} (V)	E_{max} (V)	E_{tot}	E_{ipp} (V)	Corrosion Response
316LVM;	0.08	1.60	1.36	2.96	−0.45	shiny
80 μC/cm²	1	2.18	1.64	3.74	−0.41	shiny
	4	2.71	1.41	4.12	−0.41	shiny
	7	2.36	1.81	4.17	−0.50	tarnished
	24	4.36	1.73	6.09	−0.55	roughening
	96	10.90	2.05	12.95	−0.68	scaling
	118	12.27	2.95	15.22	−1.14	dissolution
MP35N;	0.08	1.77	1.56	3.33	−1.05	shiny
80 μC/cm²	1	5.45	1.18	6.63	−0.82	tarnishing
	4	6.73	2.22	8.95	−1.18	roughening
	7	3.54	1.64	5.18	−1.09	scaling
	24	6.45	1.64	8.09	−1.00	scaling
	96	7.91	1.45	9.36	−1.18	scaling
	144	9.91	1.36	11.27	−1.18	dissolution
316LVM;	0.08	1.00	1.27	2.27	−0.22	shiny
40 μC/cm²	1	1.73	0.95	2.68	−0.23	shiny
	4	1.41	1.36	2.77	−0.23	shiny
	7	1.45	1.73	3.18	−0.23	tarnishing
	24	1.77	1.68	3.45	−0.32	tarnishing
	96	2.00	2.00	4.00	−0.27	tarnishing
	240	3.64	2.64	6.28	−0.36	tarnishing
MP35N;	0.08	0.91	1.61	2.52	−0.80	shiny
40 μC/cm²	1	2.23	1.73	3.96	−0.91	shiny
	4	2.05	2.05	4.10	−0.92	shiny
	24	4.82	2.63	7.45	−1.00	tarnishing
	120	4.45	3.00	7.45	−1.09	scaling
	144	4.45	3.09	7.54	−1.09	scaling
	240	4.46	3.00	7.46	−0.91	scaling
MP35N;	0.08	1.09	0.40	1.49	−0.25	shiny
20 μC/cm²	1	0.86	0.39	1.25	−0.18	shiny
	4	1.55	0.66	2.21	−0.41	shiny
	24	2.43	0.50	2.93	−0.61	shiny
	144	1.86	0.73	2.59	−0.41	tarnishing
	196	1.73	0.64	2.37	−0.36	roughening
	240	2.55	1.64	4.19	−0.82	roughening

Electrodes were randomly selected for duplication; similar corrosion responses resulted to those indicated in this table.

cm², E_{acc} increased the most over the course of stimulation for both alloys. Of the two alloys, the largest increases were observed for the 316LVM electrode, which increased by 0.41 V after 24 hours and then increased by an additional 2.72 V after 240 hours of stimulation. The MP35N electrode, however, increased by 1.7 V after 24 hours, but then decreased by 1.27 V. This decrease may be associated with active scaling, which may increase the surface area of the electrode. Less dramatic increases were seen in E_{acc} over the 240 hours of pulsing at 40 μC/cm² for both metals. Due to the fluctuations in E_{max}, particularly with MP35N, E_{tot} values fluctuated similarly. However, E_{tot} values clearly increased for both alloys. E_{ipp} values changed the least during stimulation compared with those of the other electrical transient components. At the lowest charge injection density of 20 μC/cm² for the MP35N electrode, the electrical transient components decreased, which correlated with the decrease in corrosion.

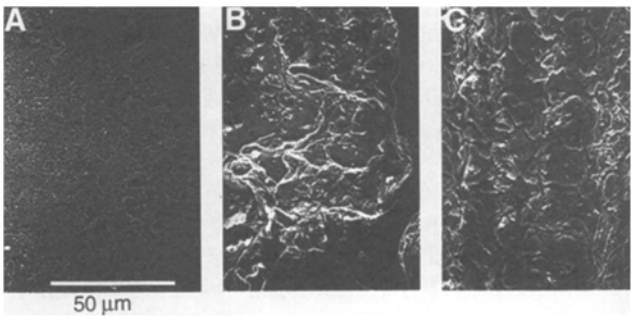

FIGURE 4. SEMs of the final corrosion responses of MP35N electrodes pulsed as indicated in Table 1 at (A) 20, (B) 40, and (C) 80 μC/cm². Roughening of the electrode's surface area is visible in (A); scaling is visible in (B); extensive roughening and scaling are visible in (C).

Access resistance (Ra) was also determined at the beginning and end of pulsing (Table 3). Ra values were calculated to be 5–10% less than expected due to the drop off in the current curve. Despite this, the response of Ra paralleled that of E_{acc} in all cases (Table 3), and increases in Ra were found to correlate well with the observed corrosion responses of the electrodes, as described in Tables 1 and 2.

TABLE 2. Electrical transients for cathodic-first pulses for 316LVM and MP35N electrodes

	Time (Hrs)	E_{acc} (V)	E_{max} (V)	E_{tot}	E_{ipp} (V)	Corrosion Response
316LVM;	0.08	−2.23	−0.91	−3.14	0.23	shiny
80 μC/cm²	1	−2.50	−1.05	−3.55	0.18	shiny
	4	−2.64	−1.27	−3.91	0.14	shiny
	24	−2.64	−1.73	−4.37	0.00	tarnishing
	144	−3.45	−1.27	−4.72	0.45	roughening
	240	−5.36	−1.18	−6.54	0.82	roughening
MP35N;	0.08	−2.05	−1.86	−3.91	0.59	shiny
80 μC/cm²	1	−2.50	−2.18	−4.68	0.73	tarnishing
	4	−2.91	−2.09	−5.00	0.77	roughening
	24	−3.82	−2.00	−5.82	0.82	scaling
	144	−3.18	−1.64	−4.82	0.68	scaling
	192	−2.18	−2.09	−4.27	0.73	scaling
	240	−2.55	−1.68	−4.23	0.68	scaling
316LVM;	0.08	−0.91	−0.86	−1.77	0.09	shiny
40 μC/cm²	1	−0.91	−0.86	−1.77	0.14	shiny
	4	−0.55	−1.27	−1.82	0.14	shiny
	24	−0.77	−1.64	−2.41	0.18	shiny
	120	−1.05	−1.05	−2.10	0.34	tarnishing
	240	−1.41	−1.18	−2.59	0.16	tarnishing
MP35N;	0.08	−1.32	−1.09	−2.41	0.14	shiny
40 μC/cm²	1	−1.18	−1.27	−2.45	0.09	shiny
	4	−1.41	−1.55	−2.96	0.36	shiny
	24	−2.45	−2.00	−4.45	0.73	tarnishing
	120	−2.55	−1.73	−4.28	0.50	roughening
	240	−2.91	−2.36	−5.27	0.73	roughening
MP35N;	0.08	−0.36	−0.86	−1.22	0.05	shiny
20 μC/cm²	1	−0.43	−0.80	−1.23	0.09	shiny
	4	−0.41	−0.93	−1.34	0.14	shiny
	24	−0.47	−1.02	−1.49	0.02	shiny
	144	−0.63	−1.32	−1.95	0.30	tarnishing
	192	−0.39	−1.45	−1.84	0.35	tarnishing
	240	−0.32	−1.39	−1.71	0.33	tarnishing

Electrodes were randomly selected for duplication; similar corrosion responses resulted to those indicated in this table.

DISCUSSION

Our principal finding was that pulsed MP35N electrodes were more susceptible to corrosion than the 316LVM electrodes. This was true for both anodic-first and cathodic-first pulsing and for different levels of charge injection. The different responses of the two electrodes were most apparent at 40 μC/cm² (Fig. 2). At this level, active corrosion was clearly visible under the light microscope for the MP35N electrodes, while the response of the 316LVM electrodes was limited to tarnishing using anodic-first pulsing. This result was somewhat surprising since MP35N has long been suggested to be more resistant to corrosion than 316LVM when used for *in vivo* implantations (11,12). These reports, however, only investigated the corrosion responses of nonstimulated MP35N and 316LVM. As a result, we investigated the effects of stimulation on these alloys for up to 240 hours of continuous pulsing at charge injections ranging from 20 to 80 μC/cm². Once the effect of stimulation was addressed, the response of these two electrode materials changed, such that MP35N was no longer superior to 316LVM.

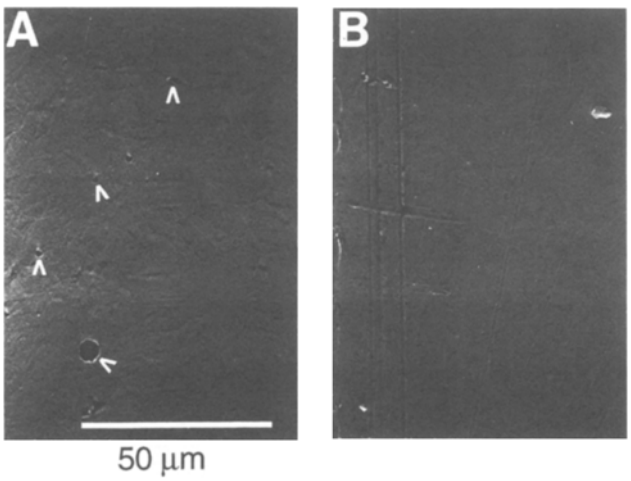

FIGURE 5. SEM comparison of the final corrosion responses of (A) MP35N and (B) 316LVM electrodes with cathodic-first pulsing at 40 μC/cm².

Accelerated corrosion of pulsed MP35N compared to 316LVM is supported by Lan *et al.*, who investigated the corrosion responses of MP35N and 316LVM electrodes with biphasic cathodic-first charge injection protocols (12). They identified the potentials at which pitting initiated for both alloys after one hour of stimulation and de-

TABLE 3. Initial and final access resistances (Ra) for both anodic-first and cathodic-first pulsing of 316LVM and MP35N electrodes

		316LVM		MP35N	
	Ra	Anodic (Ω)	Cathodic (Ω)	Anodic (Ω)	Cathodic (Ω)
80 μC/cm²	initial	95	136	102	122
	final	642	246	573	140
40 μC/cm²	initial	110	100	106	145
	final	315	144	434	265
20 μC/cm²	initial			56	169
	final			146	319

termined that the critical pitting potential of MP35N (18.8–37.5 μC/cm²) was slightly lower than that for 316LVM (37.5 μC/cm²). The two alloys were evaluated at several charge injection densities (12). At 80 μC/cm², corrosion was observed on the MP35N electrode but not on the 316LVM electrode after one hour of stimulation. These observations are in good agreement with our initial corrosion findings for the two alloys. The authors failed, however, to observe any corrosion after one hour of stimulation on either electrode material at 40 μC/cm². Based on our time course monitoring technique, one hour is a limited time period to measure the corrosion response of pulsed electrodes; longer stimulation periods are needed to determine the corrosion responses of an electrode at any given charge injection (Fig. 4).

Although it is currently believed that a charge injection density of 40 μC/cm² will prevent the onset of corrosion, this study suggests that even lower charge injection densities might be needed, especially for MP35N electrodes. Based on the amount of charge that can be injected with a metal electrode by double layer charging, 20 μC/cm² may be the maximum charge injection density possible before corrosion onset (24). Charge densities in excess of this may lead to the onset of faradaic reactions. This is clearly shown with the 316LVM electrodes, which tarnished after 240 hours of stimulation at 40 μC/cm² with either anodic-first or cathodic-first pulsing. It is not clear if a more severe corrosion response would have occurred if the electrode was stimulated longer. It is possible that the initial tarnishing could act as a passivation layer and prevent further corrosion of the 316LVM electrodes. Work is in progress to determine if longer stimulation periods (of one year for example) will produce a corrosion response beyond tarnishing.

Corrosion responses were also correlated with electrical transients (Fig. 3). Of the electrical transient components (Fig. 1), E_{acc} initiates the pulse and results from ohmic losses primarily due to the resistance of the electrode/electrolyte interface as well as the bulk electrolyte and the internal resistance of the wires. E_{acc} is also described as that potential just prior to the initiation of charge transfer (18). Generally, Ra values are used *in lieu* of E_{acc} values because of the resistive characteristics of the measurement (Table 3). As listed in Tables 1–3, E_{acc} and Ra increased during the period of pulsing more for MP35N than for 316LVM; these increases may be due to the greater build-up of surface oxides on MP35N compared with that of 316LVM. Abrupt changes in Ra were correlated with the appearance of visible corrosion products on the electrode's surface. These corrosion products may decrease the usable surface area of the electrode and may hinder the charge transfer processes at the electrode/electrolyte interface, consequently requiring a higher driving voltage from the stimulator.

During pulsing, E_{acc} is followed by E_{max} (often referred to as the polarization potential) and reflects the voltage changes at the electrode/electrolyte interface associated with charge transfer processes (18). E_{max} values versus SCE greater than 1.2 V have often been associated with corrosion responses (12). E_{max} values observed here were quite high. For example, with anodic pulsing and a charge injection density of 40 μC/cm², E_{max} values exceeded 2.5 V for both alloys. With cathodic pulsing and a charge injection of 40 μC/cm², only the MP35N alloy consistently had E_{max} values more negative than 1.2 V. We suspect that these high voltages reflect additional resistive components that develop after the initial Ra. These additional resistive components may be due to oxide build-up on the electrodes' surface. The active scaling of many of the electrodes observed here would support this view.

The third component of the electrical transient is the E_{ipp}, which occurs at the end of the interpulse period and indicates the polarization of the electrode associated with charge left on the electrodes. The changes in E_{ipp} were greater for anodic-first pulses compared with those of cathodic-first pulses. MP35N in particular had large E_{ipp}'s during 240 hours of pulsing. For example, the value of E_{ipp} for MP35N was -0.91 V compared with a value of -0.36 V for 316LVM at 40 μC/cm² for anodic-first pulsing. The increased E_{ipp} potential on the MP35N electrodes may be sufficient to promote corrosion (24).

In addition to reporting E_{acc} and E_{max}, we also reported values for E_{tot}. Changes in E_{tot} over time were found to correlate with the corrosion response of both electrodes.

E_{tot} may have applications during pulsing where a counter or SCE electrode is not available, as typically occurs with *in vivo* applications. Moreover, a clear break-off in the electrical transient that differentiates E_{acc} from E_{max} may not be apparent. In this situation, changes in E_{tot} may be correlated with corrosion of the electrode.

Corrosion responses observed here are related to charge injections and electrical transients. For 316LVM and MP35N, a passivation film is associated with corrosion resistance and is approximately 10 to 50 Å thick (3). The onset of corrosion occurs with the breakdown of this passivation layer. Factors leading to the breakdown of the passive film include a certain critical potential, the presence of damaging ions, a sufficient induction time, and the breakdown at localized sites. In addition, corrosion occurs with pulsing of these alloys when their potentials are driven to become too anodic or cathodic and the breakdown of the passive film occurs. The chemical breakdown of passivity leads to the various forms of localized corrosion, including pitting. A short pulse period (100 μsec) and a long interpulse period can provide protection against passive film breakdown. The advantage of a short pulse period is that it may not allow sufficient time for breakdown of the passivation layer. A long interpulse period can provide sufficient time for the oxide layer to undergo repair and return to its original state (12). Although a short pulse period and a long interpulse period were used in this study, both alloys were found to corrode at charge injections similar to those used in FNS applications. Of the two alloys, MP35N was found to be significantly more susceptible to pitting corrosion than was 316LVM (Fig. 5).

A concern in corrosion studies is the *in vitro* environment. This is particularly important because current methods used for *in vitro* studies fail to mimic completely the *in vivo* interstitial environment (10,17,32). In particular, oxygen concentrations in the *in vitro* environment have been shown to affect the corrosion responses of pulsed electrodes drastically (17). Yet, studies have been conducted in oxygen depleted, nitrogen rich environments (10), as well as oxygen rich, nitrogen depleted environments (17,32). Results from these studies may reflect more the effects of oxygen levels rather than the effects of pulsing. Therefore, we developed an *in vitro* environment consisting of buffered electrolytes (7) and gas concentrations (9) similar to interstitial fluid (7). The electrolyte and buffer used here are detailed in Methods. The partial pressure of interstitial oxygen is 40 mm Hg, which corresponds to 5% O_2 gas; the partial pressure of interstitial carbon dioxide is 45 mm Hg, which corresponds to 6% CO_2 gas. We recognize that our bath represents a minimal fluid and electrolyte environment. Currently, we are investigating the effects of the addition of other interstitial components including protein, sugar and urea. Another concern for mimicking the *in vivo* environment is limited fluid and electrolyte. A bath surrounds the electrode with readily diffusible fluid and electrolyte, whereas the *in vivo* environment may be better described as a moist environment with limited diffusion of fluid and electrolyte. The significance of this difference on corrosion responses of pulsed electrodes has yet to be elucidated.

Another factor possibly affecting corrosion responses in this study is the capacitor coupled discharge during the interpulse period which produces a balanced wave form. Effective discharge was assured by using a short TC of 0.96 ms. In previous work, we showed that accelerated corrosion was only observed with discharge TCs longer than 6.2 ms. Charge balance was further assured by adding a 5 KΩ resistor and diode to the output of the stimulator, which prevented discharge through the stimulator during the interpulse period.

The avoidance of electrode corrosion is an important concern for clinical applications of chronic neural prosthetics. Possible applications of epimysial and intramuscular FNS electrodes include control of upper and lower limbs and respiration, as well as management of bladder and bowel function. However, these applications depend on the stimulation demands. For example, we concluded that a larger surface area 316LVM electrode may be suitable for direct bladder stimulation for a 30-year application (13,26,28). In that study, a "woven eye" electrode configuration was satisfactory in terms of electrode migration, encapsulation, corrosion response, and fatigue failure (30). The "woven eye" configuration significantly increased the surface area of the electrode while decreasing the charge injection density, such that corrosion was not observed on "woven eye" electrodes tested after 15 hours of bipolar stimulation with 30 mA. The accelerated tests conducted in that study would be equivalent to a five-year implanted application, assuming 30 seconds of stimulation per day. An additional concern related to the corrosion response of implanted electrodes is the release of toxic compounds into the body. Iron, nickel and chromium may be released; however, preferential release of iron oxide and, to a lesser extent, nickel oxide are typically observed during corrosion (4). With the apparent slow corrosion processes seen here, the amount of metal oxides that might accompany charge injection is probably not toxic.

New multichannel stimulators will provide stimulating alternatives with electrode designs, previously unavailable, such as biphasic stimulating wave forms (31). Such capabilities allow for 1) optimizing individual electrodes, 2) limiting the stimulation field with bipolar electrode configurations and 3) reducing the rate of electrode corrosion with biphasic stimulation. For example, we observed effective stimulation with bipolar, but not monopolar, stimulation with direct bladder stimulation in an animal model. The monopolar configuration consisted of using a distant

positive electrode and a negative electrode located on the bladder wall. This configuration was not effective due to the pain response and skeletal muscle contraction along the animal's back. The bipolar configuration consisted of placing both the positive and negative electrodes on the trigone region of the bladder. It was effective with few side effects (31). Advances in stimulation, however, require electrode materials capable of withstanding the anodic pulsing necessary for bipolar stimulation. As electrode materials, 316LVM and MP35N offer the mechanical strength required for bipolar stimulation. In addition, 316LVM is readily obtainable as well as being inexpensive. However, a major concern with bipolar stimulation is the susceptibility of the electrode to pitting corrosion. Based on our findings, the MP35N electrode is more susceptible to pitting corrosion due to pulsing. As a result, we recommend using a 316LVM electrode for FNS applications requiring bipolar stimulation. However, charge injection levels should probably be kept below 40 $\mu C/cm^2$.

REFERENCES

1. Brindley, G.S.; Polkey, C.E.; Rushton, D.N. Sacral anterior root stimulators for bladder control in paraplegia. Paraplegia 20:365–381; 1982.
2. Brummer, S.B.; McHardy, J. Functional electrical stimulation: applications in neuroprosthetics. In: Hambrecht, F.T.; Reswick, J.B., eds. New York: Marcel Dekker, Inc., 1977.
3. Brummer, S.B.; McHardy, J.; Turner, M.J. Electrical stimulation with Pt electrodes: Trace analysis for dissolved platinum and other dissolved electrochemical products. Brain Behav. Evol. 14:10–22; 1977.
4. Castle, J.E.; Qui, J.H. The application of ICP-MS and XPS to studies of ion selectivity during passivation of stainless steels. J. Electrochem. Soc. 137:201–206; 1990.
5. Devine, T.M.; Wulff, J. The comparative crevice corrosion resistance of Co-Cr base surgical implant alloys. J. Electrochem. Soc. 123:1433–1437; 1976.
6. Donaldson, N.N.; Donaldson, P.E.K. When are actively balanced biphasic 'Lilly' stimulating pulses necessary in a neurological prothesis? I historical background; Pt resting potential; Q studies. Med. & Biol. Eng. Comput. 24:41–49; 1986.
7. Gamble, J.L. Chemical anatomy physiology and pathology of extracellular fluid. Massachusetts: Harvard University Press; 1954.
8. Glenn, W.W.L.; Phelps, M.L. Diaphragm pacing by electrical stimulation of the phrenic nerve. Neurosurg. 17:974–984; 1985.
9. Guyton, A.C. Transport of oxygen and carbon dioxide in the blood and body fluids. In: Textbook of medical physiology. 8th Edition. Philadelphia: W.B. Saunders Co., 1991: pp. 433–443.
10. Handa, Y.; Hoshimiya, A.; Iguchi, I.; Oda, T. Development of percutaneous intramuscular electrode for multichannel FES system. IEEE Trans. Biomed. Eng. 36:705–710; 1989.
11. Kiwerski, J.; Weiss, M.; Pasniczek R. Electro-stimulation of the median nerve in tetraplegics by means of implanted stimulators. Paraplegia 21:322–326; 1983.
12. Lan, N.L.; Daroux, M.; Mortimer, J.T. Pitting corrosion of high strength alloy stimulation electrodes under dynamic conditions. J. Electrochem. Soc. 136:947–954; 1989.
13. Lobe, G.E. Neural prosthetic interfaces with the nervous system. Trans. Neurosci. 12:195–201; 1989.
14. Man, H.C.; Gabe, D.R. A study of pitting potentials for some austentic stainless steels using a potentiodynamic technique. Corrosion Science 21:713–721; 1981.
15. McFadden, J.T. Metallurgical principles in neurosurgery. 31:373–385; 1969.
16. McHardy, J.; Geller, D.; Brummer, S.B. An approach to corrosion control during electrical stimulation. Ann. Biomed. Engin. 5:144–149; 1977.
17. McHardy, J.; Robblee, L.S.; Marston, J.M.; Brummer, S.B. Electrical stimulation with Pt electrodes. IV. Factors influencing Pt dissolution in inorganic saline. Biomat. 1: 129–134; 1980.
18. Mortimer, J.T.; Motor Prostheses. In Brookhart, J.M.; Mountcastle, V.B. eds. Handbook of physiology, Section 1: The nervous system, Vol 2. Maryland: American Physiological Society; 1981: pp 155–187.
19. Mortimer, J.T.; Kicher, T.P.; Daroux, M. Electrodes for functional neuromuscular stimulation. Fourth Progress Report, NIH Neural Prosthesis Program Contract Number N01-NS-7-2396 Applied Neural Control Laboratory, Biomedical Engineering Department, Case Western Reserve University, Cleveland, Ohio, pp. 1–30.
20. Peckner, D.; Bernstein, I.M. In Crawford, H.B.; Gatewood, B. eds. Handbook of Stainless Steel. New York: McGraw-Hill Book Co., 1977.
21. Pessall, N.; Lui, C. Determination of critical pitting potentials of stainless steel in aqueous chloride environments. Electrochimica Acta 16:x–2003; 1987.
22. Riedy, L; Walter, J; Cogan, S.; Nguyen, N.; Zaszczurynski, P. Reduced corrosion of pulsed 316LVM stainless steel electrodes by short time constant discharge. Proc. 14th Ann. Conf. IEEE Engin. Med. Biol. Soc. 14:2374–2376; 1992.
23. Robblee, L.S.; McHardy J.; Marstin, J.M.; Brummer, S.M. Electrical stimulation with Pt electrodes. V. The effect of protein on Pt dissolution. Biomaterials. 1:135–139; 1980.
24. Robblee, L.S.; Rose, T.L. In "Neural prostheses: fundamental studies" electrochemical guidelines for selection of protocols and electrode materials for neural stimulation., eds. Agnew, W.F.; McCreery, D.B. Prentice Hall, New Jersey pp. 25–66; 1990.
25. Rose, T.L.; Robblee, L.S. Electrical stimulation with Pt electrodes. VIII. Electrochemically safe charge injection limits with 0.2 ms Pulses. IEEE Trans. Biomed. Eng. 37: 1118–1120; 1990.
26. Sawan, M.; Duval, F.; Li, J.S.; Hassouna, M.; Elhilali, M.M. A new bladder stimulator-hand held controller and miniaturized implant: preliminary results in dogs. Biomed. Instr. Tech. 143–149; 1993.
27. Smith, B.T.; Mulcahey, M.J.; Triolo, R.J.; Betz, R.R. The application of a modified neuroprosthetic hand system in a child with a C7 spinal cord injury. A case report. Paraplegia 30:598–606; 1992.
28. Smith, B.T.; Peckham, P.H.; Keith, M.W.; Roscoe, D.D.

An externally powered, multichannel, implantable stimulator for versatile control of paralyzed muscle. IEEE Trans. Biomed. Eng. 34:499–508; 1987.
29. Sury, P. The comparative crevice corrosion resistance of Co-Cr base surgical implant alloys J. Electrochem. Soc. 124:869–878; 1977.
30. Walter, J.; Cogan, S.; Nguyen, N.; Robinson, C.; Dunn, B.; Zaszczurynski, P.; Wheeler, J. Evaluation of a 316LVM "woven eye" electrode for direct bladder stimulation. Proc. Ann. Conf. IEEE Eng. Med. Biol. Soc. 13:1853–1854; 1991.
31. Walter, J.S.; Wheeler, J.S.; Cogan, S.; Plishka, M.; Riedy, L.W.; Wurster, R.D. Evaluation of direct bladder stimulation with stainless steel "woven eye" electrodes. J. Urol. 1993 (In press).
32. Williams, R.L.; Brown, S.A.; Merritt, K. Electrochemical studies on the influence of proteins on the corrosion of implant alloys. Biomat. 9:181–186; 1988.